Peertechz

Head, Neck, and Oral Oncology

OPEN ACCESS

DOI: https://dx.doi.org/10.17352/hnoo

Research Article

The Value of DWI Combined with APT Imaging in the Differential Diagnosis of Parotid Tumors

Yu Feng[1], Lijun Wang[1]*, Haitao Huang[2], Lin Shi[3], Yihua Wang[4], Qin He[1] and Yihan Zhou[1]

[1]Department of Radiology, First Affiliated Hospital of Dalian Medical University, Dalian, China

[2]Department of Stomatology, First Affiliated Hospital of Dalian Medical University, Dalian, China

[3]Department of Otolaryngology, First Affiliated Hospital of Dalian Medical University, Dalian, China

[4]Department of Radiology, The Second Affiliated Hospital of Zhejiang University of Traditional Chinese Medicine, Zhejiang, China

submitted : 26 October, 2026
Accepted : 06 November, 2026
Published : 07 November, 2026

***Corresponding author:** Lijun Wang, Department of Radiology, First Affiliated Hospital of Dalian Medical University, Dalian, China, E-mail: wanglj345@163.com

Keywords: Parotid gland tumor; Diffusion-weighted imaging; Amide proton transfer-weighted imaging; Magnetic resonance imaging

Copyright License: © 2026 Feng Y, et al. This is an open-access article distributed under the terms of the Creative Commons Attribution License, which permits unrestricted use, distribution, and reproduction in any medium, provided the original author and source are credited.

https://www.organscigroup.us

Check for updates

Abstract

Objective: To investigate the value of Diffusion-Weighted Imaging (DWI) combined with Amide Proton Transfer Weighted Imaging (APTw) sequences in the diagnosis of parotid tumors.

Methods: A retrospective analysis was conducted on 80 patients with parotid gland solid tumors who underwent 3.0T MRI examinations at our institution and received pathological confirmation. 62 cases of Benign Tumors (BT), 18 cases of Malignant Tumors (MT). Logistic regression was used to analyze statistically significant parameters and their combined diagnostic models. The DeLong test was applied to compare differences in area under the Receiver Operating Characteristic (ROC) curve.

Results: DeLong's test indicated that for distinguishing Pleomorphic Adenoma (PA) from Warthin's Tumor (WT), both ADC values and their combination yielded AUCs significantly greater than APT values ($P<0.05$). In differentiating PA from MT, the combined AUC was significantly greater than that of APT alone ($P<0.05$). No correlation was observed between ADC and APT values.

Conclusion: DWI and APT can provide quantitative assessment of the characteristics of parotid gland tumors. The combined use of ADC and APT imaging demonstrated promising diagnostic potential for distinguishing PA from WT, and also from MT. Specifically, when distinguishing PA from MT, the combined model achieved a high AUC value. APT can distinguish WT from MT; however, the combined application did not improve its diagnostic performance.

Background

Salivary gland tumors are relatively rare among head and neck tumors, accounting for approximately 6% of all head and neck tumors. As the largest salivary gland, the parotid gland is the site of origin for about 80% of salivary gland tumors [1]. According to the 5th edition of the World Health Organization (WHO) Classification of Tumors of the Head and Neck, benign salivary gland tumors comprise 15 distinct types, while malignant salivary gland tumors number more than 20 [2]. Parotid gland tumors exhibit a wide variety of histological types, and their benign and malignant lesions often overlap in clinical presentation, laboratory findings, and conventional imaging features, making accurate differentiation a significant challenge in clinical practice.

Treatment strategies for parotid gland tumors vary depending on the type [3]. MT typically requires total parotidectomy, supplemented with radiation therapy as indicated. Among BT, PA carries a risk of local recurrence and even malignant transformation, so parotid superficial lobe resection or total parotidectomy is often performed [4];

Citation: Feng Y, Wang L, Huang H, Shi L, Wang Y, He Q, et al. The Value of DWI Combined with APT Imaging in the Differential Diagnosis of Parotid Tumors. Head Neck Oral Oncol. 2026;2(1):1-7. Available from:: https://dx.doi.org/10.17352/hnoo.000002

in contrast, WT has a low rate of malignant transformation and is typically managed with conservative observation [3]. Therefore, accurate preoperative determination of the tumor's nature is crucial for developing an appropriate treatment plan.

Currently, Fine Needle Aspiration Cytology (FNAC) is commonly used in clinical practice for preoperative differential diagnosis; however, this method carries risks such as tumor cell implantation and metastasis, as well as stimulation of tumor proliferation [5,6], and may yield false-negative results [7,8]. Although ultrasound is simple and non-invasive, its ability to distinguish the histological types of parotid tumors is limited [9,10]. Similarly, conventional CT and MRI sequences often exhibit significant overlap in imaging features across different tumor types. As demonstrated by the findings of Karaman et al. [11], accurate histological diagnosis based solely on conventional MRI features is challenging, as there is significant overlap in capsule characteristics and signal intensity between BT and MT.

In recent years, functional MRI sequences have demonstrated higher accuracy and sensitivity in the differential diagnosis of parotid tumors, providing an important reference for clinical classification. DWI can quantitatively assess the degree of water diffusion restriction within tissues; however, because WT has a higher cellular density, relying solely on DWI to distinguish between WT and MT may have limitations [12]; APTw is based on the chemical exchange saturation transfer mechanism and reflects the metabolic level of tumor cells by detecting the content of free proteins within the tumor [13]. This study aims to investigate the value of combining DWI and APTw imaging in the differential diagnosis of parotid gland tumor subtypes, with the goal of providing imaging evidence to support clinical decision-making.

Materials and methods

Participants

The institutional review board of our hospital approved our retrospective study (license number: PJ-KS-KY-2026-248). The patients who participated in this study provided their written informed consent. From April 2019 to December 2024, the First Affiliated Hospital of Dalian Medical University treated 80 patients with parotid tumors, including 53 males and 27 females; their ages ranged from 24 to 85 years (mean 56.00 ± 14.03 years); Among them, 38 cases of PA, including 21 males and 17 females; 24 cases of WT, including 21 males and 3 females; 18 cases of MT (including 3 cases of squamous cell carcinoma, 2 cases of acinic cell carcinoma, 2 cases of adenoid cystic carcinoma, 2 cases of mucoepidermoid carcinoma, 2 cases of basal cell adenocarcinoma, 2 cases of malignant transformation of neurofibroma, 2 cases of lymphoma, 1 case of secretory carcinoma, 1 case of epithelio-myoepithelial carcinoma, and 1 case of ductal adenocarcinoma), 12 men and 6 women. Inclusion criteria: (1) Complete clinical information; tumor type confirmed by surgical pathology; and no history of parotid gland-related diseases. (2) No contraindications for MRI; a 3.0T MRI scan must be performed prior to treatment (scan sequences must include conventional MR sequences, DWI, and APT sequences). Exclusion Criteria: (1) Severe MRI artifacts that interfere with data measurement. (2) The solid component of the parotid tumor is too small.

Methods

All 80 patients underwent conventional MRI, DWI, and APT scans. A 3.0T Ingenia MRI scanner (Philips, Netherlands) and a combined head-neck coil were used, with patients positioned supine in a head-first configuration. DWI: TR = 4936 ms, TE = 58 ms, FOV 200 mm × 200 mm × 89 mm, b-value 0, 1000 s/mm², voxel size 2 mm × 2.5 mm × 4 mm, matrix size 100 × 80 × 18, number of excitation pulses 2, acquisition time 138 s. APT: TR = 5864 ms, TE = 8.3 ms, FOV = 230 mm × 180 mm × 70 mm, voxel size = 1.8 mm × 1.8 mm × 7 mm, matrix size 128 × 100 × 10, number of excitation pulses 1, acquisition time 217 s.

For image analysis and data processing, the acquired images are transferred to the Intellispace Portal (ISP) 9.0 post-processing workstation (Philips, Netherlands). Using conventional T2-weighted images (T2WI) as a reference, the slice with the largest area of solid tumor component was selected, avoiding areas of intratumoral necrosis, cystic changes, and hemorrhage. Individual regions of interest (ROIs) were manually delineated on ADC maps and APT pseudocolor maps for the three tumor types (Figure 1). Two radiology

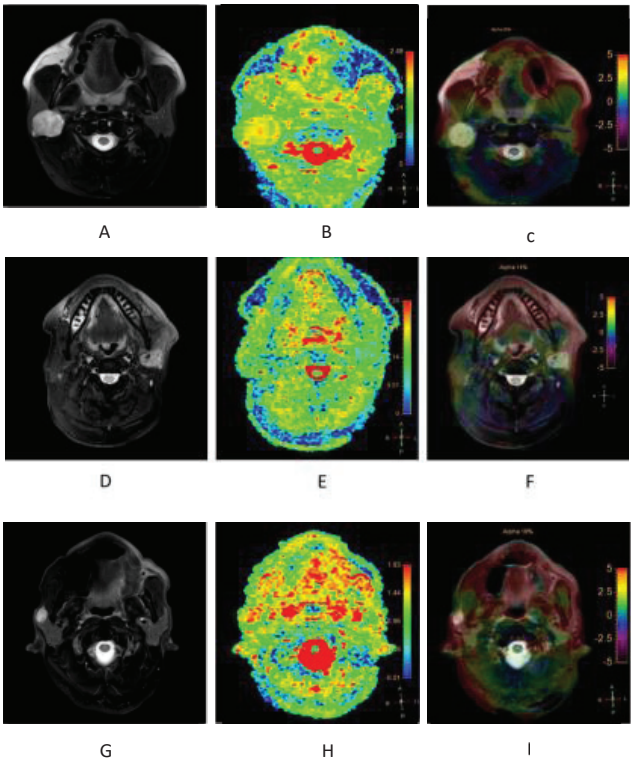


Figure 1: A 32-year-old male with PA of the right parotid gland, axial T2-weighted image (A); ADC map, with a value of 2 x 10^-3 mm2/s (B); APTw image (fused with the T2 - weighted image), with a value of 2.57 (C).
A 62-year-old male with WT of the left parotid gland, axial T2-weighted image (D); ADC map, with a value of 0.74 x10-3 mm2/s (E); APTw image (fused with the T2 - weighted image), with a value of 2.3 (F).
A 61-year-old male with acinar cell carcinoma of the right parotid gland, axial T2-weighted image (G); ADC map, with a value of 1.68 x 10^-3 mm2/s (H); APTw image (fused with the T2-weighted image), with a value of 5.6 (I).

Citation: Feng Y, Wang L, Huang H, Shi L, Wang Y, He Q, et al. The Value of DWI Combined with APT Imaging in the Differential Diagnosis of Parotid Tumors. Head Neck Oral Oncol. 2026;2(1):1-7. Available from:: https://dx.doi.org/10.17352/hnoo.000002

residents each performed two independent measurements, and the consistency of their results was analyzed. Ultimately, the mean of the measurements taken by the first resident was used for statistical analysis.

Statistical analysis

Statistical analysis was performed using R software (version 4.3.3, www.R-project.org). Quantitative data following a normal distribution are expressed as mean ± standard deviation (x ± s). For comparisons among multiple groups, one-way analysis of variance (ANOVA) was used, and pairwise comparisons between groups were performed using the LSD test. The Intraclass Correlation Coefficient (ICC) was used to evaluate the agreement between measurements by two physicians; an ICC > 0.75 was considered good agreement. Logistic regression was used to analyze parameters with statistically significant differences and to develop combined diagnostic models; ROC curves were plotted to evaluate the diagnostic performance of ADC values, APT values, and their combination in distinguishing parotid tumors, with AUC comparisons performed using the DeLong test; the significance level was set at $\alpha = 0.05$. Spearman's correlation analysis was used to assess whether there was a correlation between ADC and APT values; a $|\rho|$ value of <0.3 indicates a non-linear relationship.

Results

Inter-rater agreement between two physicians in measuring ADC and APT values for parotid tumors: The inter-rater agreement between the two physicians in measuring ADC and APT values for parotid tumors was good (ICC > 0.75).

Comparison of ADC and APT values for three types of parotid gland tumors: The ADC values for WT and MT were both lower than those for PA; the APT values for PA and WT were both lower than those for MT. The ADC values, from highest to lowest, were PA, MT, and WT. The APT values, from highest to lowest, were MT, WT, and PA. (Table 1, Figure 2).

ROC Curve Analysis of ADC, APT, and Their Combination for the Differential Diagnosis of Parotid Tumors: Using an ADC cutoff value of 0.77 × 10^{-3} mm^2/s to distinguish PA from MT yielded an AUC of 0.879, with a sensitivity of 83.3% and a specificity of 94.7%; combining APT increased the AUC to 0.977; Using an APT cutoff of 3.20 to distinguish WT from MT yielded an AUC of 0.700; after combining the two, the AUC decreased to 0.698, but both values were higher than the AUC of 0.656 obtained by using ADC values alone to distinguish between the two; however, there was no statistically significant difference in AUC between the ADC values and the combined ADC-APT values for the PA and MT groups; There was no statistically significant difference in the AUC of the APT values for the WT and MT groups compared to the combined AUC (Table 2, Figure 3). There was no correlation between ADC values and APT values ($r = -0.163$, $P > 0.05$; Figure 4).

Discussion

This study aimed to evaluate the diagnostic performance of ADC values, APT values, and their combined application in distinguishing subtypes of parotid tumors, with the goal of providing imaging evidence to support the development of individualized preoperative treatment plans and postoperative follow-up strategies for patients. The results showed significant differences in ADC and APT values among different subtypes of parotid tumors, specifically with PA exhibiting the highest ADC values and MT exhibiting the highest APT values. Regarding the differentiation between PA and MT, although the AUC of the combined model was numerically superior to that of the single-sequence model, the difference was at the statistical threshold, which may be attributed to the small sample size.

From a pathological perspective, the histological structure of PA is relatively complex, consisting primarily of epithelial, mucoid, and chondroid tissues, and is typically characterized by a low cell-to-stroma ratio. This heterogeneity and relatively low cell density result in PA typically having a high ADC value [14] and a relatively low APT value. As the most common BT of the parotid gland, PA's incomplete capsule and cell-to-stroma ratio are closely associated with the risk of recurrence [15]. These factors can lead to varying pathological features within PA, resulting in statistically significant differences in ADC

Table 1: Comparison of ADC and APT values for three types of parotid gland tumors (x ± s)

Type	Number of patients	ADC/(x10^{-3} mm^2/s)	APT
PA	38	1.71±0.28	2.56±0.59[c]
WT	24	1.10±0.46[a]	3.02±0.73[c]
MT	18	1.18±0.34[a]	3.67±0.93

Note: a compared with PA, P < 0.001; b compared with WT, P < 0.001; c compared with MT, P < 0.05

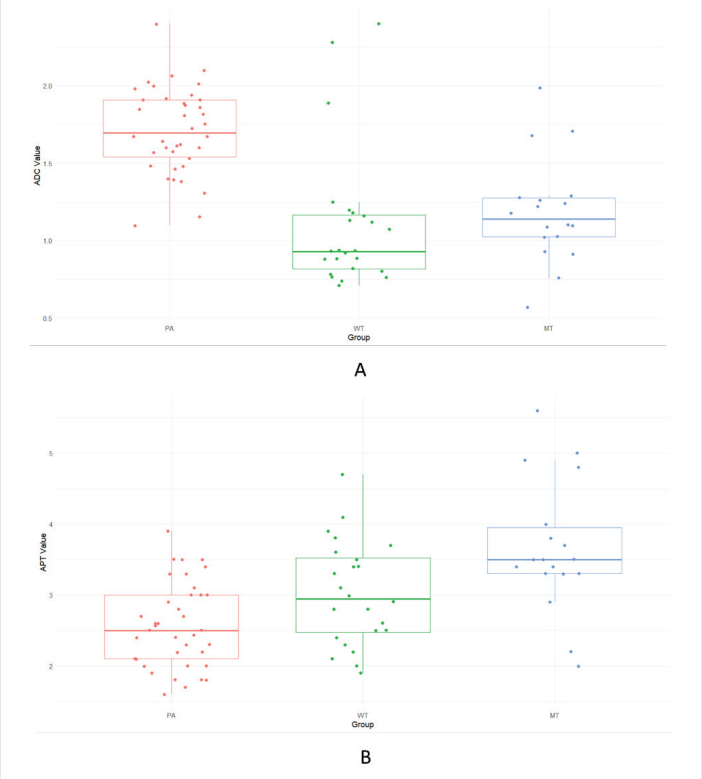


Figure 2: Box plot of ADC values for three types of parotid gland tumors (A); box plot of APT values for three types of parotid gland tumors (B).

Citation: Feng Y, Wang L, Huang H, Shi L, Wang Y, He Q, et al. The Value of DWI Combined with APT Imaging in the Differential Diagnosis of Parotid Tumors. Head Neck Oral Oncol. 2026;2(1):1-7. Available from:: https://dx.doi.org/10.17352/hnoo.000002

Table 2: ADC Values, APT Values, and the Diagnostic Performance of Combined ADC and APT Values in the Differential Diagnosis of Parotid Tumors

Parameters	Cut-off value	Sensitivity /%	Specificity/%	Jorden Index	Area under the curve	95%CI	P-value
PA vs WT							
ADC	0.78x10^{-3} mm^2/s	0.875	0.947	0.822	0.878[a]	0.759~0.997	0.031
APT	2.75	0.625	0.658	0.283	0.679[b]	0.542~0.816	0.021
ADC+APT	0.44	0.875	0.921	0.796	0.882[c]	0.764~1.00	0.754
PA vs MT							
ADC	0.77x10^{-3} mm^2/s	0.833	0.947	0.781	0.879[a]	0.765~0.993	0.748
APT	3.20	0.833	0.816	0.649	0.848[b]	0.731~0.965	0.022
ADC+APT	0.72	0.833	1.000	0.833	0.977[c]	0.944~1.000	0.060
WT vs MT							
ADC	0.98x10^{-3} mm^2/s	0.778	0.583	0.361	0.656[a]	0.485~0.828	0.720
APT	3.20	0.833	0.583	0.417	0.700[b]	0.538~0.863	0.851
APT+ADC	0.39	0.833	0.583	0.417	0.698[c]	0.535~0.861	0.719

Note: a Compared to APT; b Compared to the combination; c Compared to ADC

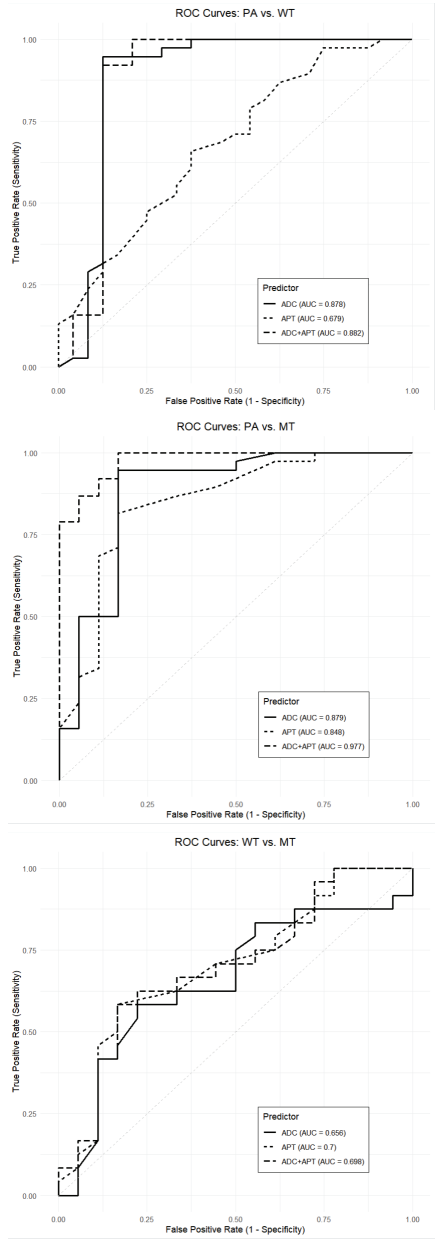


Figure 3: ROC curves for ADC values, APT values, and the combined use of both in the differential diagnosis of parotid tumors.

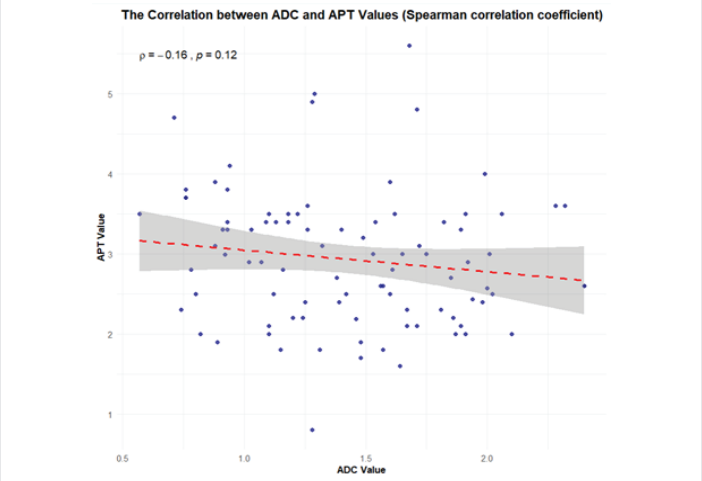


Figure 4: Scatter plot showing the correlation between ADC and APT values.

values. Recently, several studies have focused on the subtyping of PA to more accurately assess the efficacy of ADC values in distinguishing PA subtypes. Mai et al. [16] constructed a decision tree using conventional imaging features combined with ADC radiomics to predict high-risk capsular characteristics of PA, thereby aiding in the formulation of preoperative surgical plans and the arrangement of follow-up strategies. Monestier et al. [17] found that ADC values in the low-cell subtype of PA were higher than in other subtypes, suggesting that ADC values may aid in the preoperative classification of PA subtypes. In the future, the potential of APT values in distinguishing PA subtypes may be explored. In contrast, WT consists of glandular epithelium and a lymphocyte-rich stroma, with a high cell-to-stroma ratio and lymphocytic infiltration, resulting in more pronounced diffusion restrictions; consequently, the ADC values for WT are typically lower than those for PA. Consistent with previous studies [12,18], this study found a statistically significant difference in ADC values between these two tumor types.

The pathological characteristics of MT are even more complex. Typically, MT exhibit low ADC values and high

Citation: Feng Y, Wang L, Huang H, Shi L, Wang Y, He Q, et al. The Value of DWI Combined with APT Imaging in the Differential Diagnosis of Parotid Tumors. Head Neck Oral Oncol. 2026;2(1):1-7. Available from:: https://dx.doi.org/10.17352/hnoo.000002

APT values due to their high rate of cell proliferation, dense cellular arrangement, and frequent presence of necrosis and high protein content. Low ADC values reflect restricted diffusion, while high APT values indicate more active cellular metabolism and protein synthesis. This study included non-epithelial MT, such as lymphoma, in the MT group. Their unique histological structures increased the variability of ADC values within the MT group, posing a challenge to the discriminatory ability of a single parameter. This heterogeneity of MT, coupled with limitations in sample size, represents a common challenge currently faced by deep learning models in the classification of parotid tumors [19]; further improvements in model performance depend on expanding the sample size of malignant cases and multi-center collaboration.

APTw imaging technology is limited by its relatively low spatial resolution, and the tissues surrounding the parotid gland (such as bones and ear structures) cause extreme non-uniformity in the B0 magnetic field; the resulting high signal may interfere with the accurate measurement of APTw values in the lesion [20]. Therefore, this study employs a method of fusing T2WI and APT images to achieve more precise delineation of the lesion area, thereby minimizing measurement errors caused by artifacts and other factors. Although the study by Wang et al. [21] was limited to analysis at the level of the largest lesion due to measurement efficiency constraints, it noted that APTmax may represent the highest metabolic level of the tumor and offers certain advantages in assessing tumor heterogeneity; furthermore, whole-volume assessment may more comprehensively capture the biological characteristics of parotid tumors. However, the single, localized ROI delineation method used in this study has significant limitations regarding tumor heterogeneity, particularly for PA with diverse components and WT with cystic changes.

The experimental results showed that the APT values for parotid gland MT were the highest across all groups, consistent with previous studies [22,23]; however, these values exhibited significant variability, which may be attributed to the limited sample size of MT cases included in this study and the diverse range of histological subtypes. Further analysis revealed that the APT values for acinar cell carcinoma and secretory carcinoma were higher than those for other MT subtypes. Secretory carcinomas often contain abundant eosinophilic cytoplasm [2], suggesting the presence of a large amount of protein secretions within them; in contrast, acinar cell carcinomas are characterized by cytoplasmic granules rich in proenzymes [24], which similarly lead to elevated protein levels within the tumor cells. This may constitute the pathological basis for their higher APT values. However, this is only a preliminary observation based on a small sample size; further validation requires subtype analysis using a larger sample size. Furthermore, in MT, the mismatch between cell proliferation rates and neovascularization makes cystic changes and areas of necrosis more likely to occur. In their study of gliomas, Togao et al. [25] noted that APT signal intensity is not only positively correlated with tumor cell density, but that fluid accumulation in areas of micro-necrosis or micro-cystic changes can also lead to elevated APT signals; this mechanism may also apply to parotid MT.

In the DWI imaging used in this study, ADC values demonstrated a certain degree of discriminatory ability in distinguishing PA from WT and MT. In distinguishing between PA and MT, the combined model yielded a numerically higher AUC; however, due to the small sample size of MT in this study, the DeLong test failed to confirm that the difference between the two groups was statistically significant. Further validation of this improved performance is needed in large-scale, multicenter cohorts. Furthermore, due to the high density of WT cells, ADC values are unable to effectively distinguish between WT and MT. In contrast, APT imaging has demonstrated higher sensitivity in distinguishing between the two; however, current data are insufficient to prove that APT provides significant additional diagnostic value over ADC. In head and neck tumors, with the exception of thyroid tumors [26,27], most studies indicate that APT values in MT are higher than those in benign tumors [28], and the results of this study are consistent with this finding.

The main limitations of this study are as follows: (1) The pathological types of MT are diverse, and the overall sample size is small. (2) The method used for delineating ROI has limitations, as it overlooks tumor heterogeneity. (3) The BT group was not included due to the small number of cases of basal cell adenomas; future studies should be conducted at multiple centers to expand the sample size and conduct a comprehensive investigation.

In this study, the combined use of ADC and APT imaging improved the ability to distinguish between PA and WT, as well as between PA and MT; however, no significant improvement was observed in distinguishing other tumor subtypes. At the same time, the study indicated that there was no correlation between ADC values and APT values, suggesting that the two imaging sequences provide different information and that their combined use allows for tumor assessment from different perspectives. However, based on the APT measurement data, the differences in APT values among the three tumor subtypes were small, and the standard deviations within each group were large. This indicates a high degree of overlap in APT values across these subtypes and limited discriminatory power, which may be one of the reasons for its low diagnostic efficacy in subtype differentiation. Further research could be conducted by increasing the sample size.

Conclusion

DWI and APT can quantitatively assess the characteristics of parotid gland tumors; PA has the highest ADC value and the lowest APT value, while WT has the lowest ADC value and MT has the highest APT value. The APT value can be used to distinguish between WT and MT. The AUC value for the combined multiparametric diagnosis of PA and MT is high, indicating good diagnostic performance.

Citation: Feng Y, Wang L, Huang H, Shi L, Wang Y, He Q, et al. The Value of DWI Combined with APT Imaging in the Differential Diagnosis of Parotid Tumors. Head Neck Oral Oncol. 2026;2(1):1-7. Available from:: https://dx.doi.org/10.17352/hnoo.000002

Table S1: The comprehensive model parameters and specifications for the combined models.

	Outcome Encoding (0/1)	Predictor Handling (Units)	Variable (Term)	β Coefficient (Estimate)	SE	z value	P value	OR (95% CI)	Probability Cut-off
PA vs WT	PA = 0 WT = 1	Continuous, unstandardized (ADC:×10−3mm2/s, APT: %)	Intercept ADC APT	3.436 -4.169 0.734	*1.968* *1.018* *0.559*	*1.746* *-4.095* *1.314*	*0.081* *<0.001* *0.189*	— 0.015 (0.002–0.114) 2.084 (0.697–6.230)	0.509
PA vs MT	PA = 0 MT = 1	Continuous, unstandardized (ADC:×10−3mm2/s, APT: %)	Intercept ADC APT	3.190 -8.706 2.849	3.345 2.940 0.949	0.954 -2.961 3.003	0.340 0.003 0.003	— 0.0002 (<0.001–0.052) 17.271 (2.680–111.315)	0.717
WT vs MT	WT = 0 MT = 1	Continuous, unstandardized (ADC:×10−3mm2/s, APT: %)	Intercept ADC APT	-4.890 0.412 1.270	2.010 0.851 0.516	-2.433 0.484 2.460	0.015 0.628 0.014	— 1.510 (0.285–8.003) 3.561 (1.294–9.799)	0.388

Note: 0 indicates a reference value/negative result; 1 indicates a positive result

References

1. Szydłowski K, Puchalski M, Ołdziej S, Kasprzyk-Tryk A, Skorek A, Tretiakow D. The impact of inflammation on the etiopathogenesis of benign salivary gland tumors: a scoping review. Int J Mol Sci. 2024;25(23):12558. Available from: https://doi.org/10.3390/ijms252312558
2. Skálová A, Hyrcza MD, Leivo I. Update from the 5th Edition of the World Health Organization Classification of Head and Neck Tumors: salivary glands. Head Neck Pathol. 2022;16:40-53. Available from: https://doi.org/10.1007/s12105-022-01420-1
3. Gökçe E. Multiparametric magnetic resonance imaging for the diagnosis and differential diagnosis of parotid gland tumors. J Magn Reson Imaging. 2020;52:11-32. Available from: https://doi.org/10.1002/jmri.27061
4. Hellquist H, Paiva-Correia A, Vander Poorten V, Quer M, Hernandez-Prera JC, Andreasen S, et al. Analysis of the clinical relevance of histological classification of benign epithelial salivary gland tumours. Adv Ther. 2019;36:1950-1974. doi Available from: https://doi.org/10.1007/s12325-019-01007-3
5. Mezei T, Mocan S, Ormenisan A, Baróti B, Iacob A. The value of fine needle aspiration cytology in the clinical management of rare salivary gland tumors. J Appl Oral Sci. 2018;26:e20170267. Available from: https://doi.org/10.1590/1678-7757-2017-0267
6. Mantopoulos K, Sievert M, Iro A, Müller SK, Koch M, Schapher M, et al. Histopathological comparison of pleomorphic adenomas of the parotid and submandibular gland. Oral Dis. 2022;28:1131-1136. Available from: https://doi.org/10.1111/odi.13858
7. Tan LG, Khoo ML. Accuracy of fine needle aspiration cytology and frozen section histopathology for lesions of the major salivary glands. Ann Acad Med Singap. 2006;35:242-248. Available from: 10.47102/annals-acadmedsg.V35N4p242.
8. Eytan DF, Yin LX, Maleki Z, Koch WM, Tufano RP, Eisele DW, et al. Utility of preoperative fine needle aspiration in parotid lesions. Laryngoscope. 2018;128:398-402. Available from: https://doi.org/10.1002/lary.26776
9. Zengel P, Notter F, Clevert DA. Does acoustic radiation force elastography improve the diagnostic capability of ultrasound in the preoperative characterization of masses of the parotid gland? Dentomaxillofac Radiol. 2018;47:20180068. Available from: https://doi.org/10.1259/dmfr.20180068
10. Zhang YF, Li H, Wang XM, Cai YF. Sonoelastography for differential diagnosis between malignant and benign parotid lesions: a meta-analysis. Eur Radiol. 2019;29:725-735. Available from: https://doi.org/10.1007/s00330-018-5609-6
11. Karaman CZ, Tanyeri A, Özgür R, Öztürk VS. Parotid gland tumors: comparison of conventional and diffusion-weighted MRI findings with histopathological results. Dentomaxillofac Radiol. 2021;50:20200391. Available from: https://doi.org/10.1259/dmfr.20200391
12. Yologlu Z, Aydin H, Alp NA, Aribas BK, Kizilgoz V, Arda K. Diffusion-weighted magnetic resonance imaging in the diagnosis of parotid masses: preliminary results. Saudi Med J. 2016;37:1412-1416. Available from: https://doi.org/10.15537/smj.2016.12.16288
13. Wang Y, Wang L, Huang H, Ma J, Lin L, Liu L, et al. Amide proton transfer-weighted magnetic resonance imaging for the differentiation of parotid gland tumors. Front Oncol. 2023;13:1223598. Available from: https://doi.org/10.3389/fonc.2023.1223598
14. Abend A, Keir G, Krishnan K, Kim J, Strauss S, Kutler D. Parotid pleomorphic adenoma and apparent diffusion coefficient: a novel clinical prediction tool. Laryngoscope. 2025;135:3703-3711. Available from: https://doi.org/10.1002/lary.32276
15. Dulguerov P, Todic J, Pusztaszeri M, Alotaibi NH. Why do parotid pleomorphic adenomas recur? A systematic review of pathological and surgical variables. Front Surg. 2017;4:26. Available from: https://doi.org/10.3389/fsurg.2017.00026
16. Mai W, Tan J, Zhang L, Wang L, Zhang D, Shi C, et al. Predicting high-risk capsular features in pleomorphic adenoma of the parotid gland through a nomogram model based on ADC imaging. Acad Radiol. 2024;31:4408-4418. Available from: https://doi.org/10.1016/j.acra.2024.06.003
17. Monestier L, Del Grande J, Haddad R, Santini L, Michel J, Varoquaux A, et al. Correlation between MRI (DWI and DCE) and cellularity of parotid gland pleomorphic adenomas. Eur Arch Otorhinolaryngol. 2024;281:2655-2665. Available from: https://doi.org/10.1007/s00405-024-08562-8
18. Kato H, Kawaguchi M, Ando T, Shibata H, Ogawa T, Noda Y, et al. Current status of diffusion-weighted imaging in differentiating parotid tumors. Auris Nasus Larynx. 2023;50:187-195. Available from: https://doi.org/10.1016/j.anl.2022.07.002
19. Liu X, Pan Y, Zhang X, Sha Y, Wang S, Li H, et al. A deep learning model for classification of parotid neoplasms based on multimodal magnetic resonance image sequences. Laryngoscope. 2023;133:327-335. Available from: https://doi.org/10.1002/lary.30154
20. Chen Y, Wang X, Su T, Xu Z, Wang Y, Zhang Z, et al. Feasibility evaluation of amide proton transfer-weighted imaging in the parotid glands: a strategy to recognize artifacts and measure APT value. Quant Imaging Med Surg. 2021;11:2279-2291. Available from: https://doi.org/10.21037/qims-20-675
21. Wang Y, Wang L, Huang H, Ma J, Lin L, Liu L, et al. Amide proton transfer-weighted magnetic resonance imaging for the differentiation of parotid gland tumors. Front Oncol. 2023;13:1223598. Available from: https://doi.org/10.3389/fonc.2023.1223598
22. Kamitani T, Sagiyama K, Togao O, Yamasaki Y, Hida T, Matsuura Y, et al. Amide proton transfer (APT) imaging of parotid tumors: differentiation of malignant and benign tumors. Eur J Radiol. 2020;129:109047. Available from: https://doi.org/10.1016/j.ejrad.2020.109047

Citation: Feng Y, Wang L, Huang H, Shi L, Wang Y, He Q, et al. The Value of DWI Combined with APT Imaging in the Differential Diagnosis of Parotid Tumors. Head Neck Oral Oncol. 2026;2(1):1-7. Available from:: https://dx.doi.org/10.17352/hnoo.000002

23. Bae YJ, Choi BS, Jeong WJ, Jung YH, Park JH, Sunwoo L, et al. Amide proton transfer-weighted MRI in the diagnosis of major salivary gland tumors. Sci Rep. 2019;9:8349. Available from: https://doi.org/10.1038/s41598-019-44820-0

24. Kirschnick LB, Silveira FM, Schuch LF, Fonseca FP, Martins MAT, Lopes MA, et al. Clinicopathological analysis of oral and maxillofacial acinic cell carcinoma: a systematic review. J Oral Pathol Med. 2021;50:741-749. Available from: https://doi.org/10.1111/jop.13159

25. Togao O, Yoshiura T, Keupp J, Hiwatashi A, Yamashita K, Kikuchi K, et al. Amide proton transfer imaging of adult diffuse gliomas: correlation with histopathological grades. Neuro Oncol. 2014;16:441-448. Available from: https://doi.org/10.1093/neuonc/not158

26. Liu R, Jiang G, Gao P, Li G, Nie L, Yan J, et al. Non-invasive amide proton transfer imaging and ZOOM diffusion-weighted imaging in differentiating benign and malignant thyroid micronodules. Front Endocrinol (Lausanne). 2018;9:747. Available from: https://doi.org/10.3389/fendo.2018.00747

27. Li G, Jiang G, Mei Y, Gao P, Liu R, Jiang M, et al. Applying amide proton transfer-weighted imaging (APTWI) to distinguish papillary thyroid carcinomas and predominantly solid adenomatous nodules: comparison with diffusion-weighted imaging. Front Oncol. 2020;10:918. Available from: https://doi.org/10.3389/fonc.2020.00918

28. Yuan J, Chen S, King AD, Zhou J, Bhatia KS, Zhang Q, et al. Amide proton transfer-weighted imaging of the head and neck at 3 T: a feasibility study on healthy human subjects and patients with head and neck cancer. NMR Biomed. 2014;27:1239-1247. Available from: https://doi.org/10.1002/nbm.3184

Discover a bigger Impact and Visibility of your article publication with Peertechz Publications

Highlights

- Signatory publisher of ORCID
- Signatory Publisher of DORA (San Francisco Declaration on Research Assessment)
- Articles archived in worlds' renowned service providers such as Portico, CNKI, AGRIS, TDNet, Base (Bielefeld University Library), CrossRef, Scilit, J-Gate etc.
- Journals indexed in ICMJE, SHERPA/ROMEO, Google Scholar etc.
- OAI-PMH (Open Archives Initiative Protocol for Metadata Harvesting)
- Dedicated Editorial Board for every journal
- Accurate and rapid peer-review process
- Increased citations of published articles through promotions
- Reduced timeline for article publication

Submit your articles and experience a new surge in publication services
https://www.peertechzpublications.org/submission

Peertechz journals wishes everlasting success in your every endeavours.

Citation: Feng Y, Wang L, Huang H, Shi L, Wang Y, He Q, et al. The Value of DWI Combined with APT Imaging in the Differential Diagnosis of Parotid Tumors. Head Neck Oral Oncol. 2026;2(1):1-7. Available from:: https://dx.doi.org/10.17352/hnoo.000002